Int. J. of GEOMATE, Dec, 2013, Vol. 5, No. 2 (Sl. No. 10), pp. 743-748
Geotec., Const. Mat. & Env., ISSN:2186-2982(P), 2186-2990(O), Japan

IDENTIFYING SOLUTE DISPERSIVITY IN UNSATURATED POROUS MEDIA USING A NON-INTRUSIVE TECHNIQUE

Kazuya Inoue[1], Takayuki Fujiwara[1] and Tsutomu Tanaka[1]

[1] Graduate School of Agricultural Science, Kobe University, Japan

ABSTRACT: A non-intrusive methodology using spatial moment analysis linked with image processing of a dye tracer behavior in porous media was applied to identify time-series variation of dispersivities not only in longitudinal but in transverse directions under saturated and unsaturated conditions. Dye tracer experiments were carried out in a two-dimensional and vertically placed water tank with the dimensions of 100 cm width, 100 cm height and 3 cm thickness under saturated and unsaturated flow conditions. An image processing technique based on digitalized spatial distributions of dye tracer allowed to link with a spatial moment approach to identify the temporal change of the longitudinal and transverse dispersivities. Dispersivities exhibited an increasing and decreasing tendency associated with infiltration rates and showed a marked difference between estimates under saturated and unsaturated conditions. Transverse dispersivities under unsaturated conditions were approximately one order larger than those under saturated conditions. This attributed to the effect of air distributions in porous media on the temporal and spatial change of solute dispersion phenomena.

Keywords: Solute dispersivity, Unsaturated porous media, Spatial moment, Image analysis, Dye

1. INTRODUCTION

Fertilizers and pesticides have ensured high productivity of agriculture and a quality supply of food in past decades. However, use of fertilizers and pesticides can raise concerns about health risks from residues in food and drinking water such as methemoglobinemia and neurodegenerative disorders like Parkinson [1], [2]. Fast transport of fertilizers and other agrochemicals into subsurface or groundwater systems has been recognized as a serious threat due to high concentration of solutes. Thus, an understanding of solute transport mechanism through not only saturated but unsaturated zones under various hydraulic conditions is important in environmental protection and agricultural activity.

In order to understand and express the transport behavior of contaminants in a subsurface, the transport parameters such as longitudinal and transverse dispersivities are some of the key factors that play an important role in spreading the contaminants. Several studies have been conducted through column experiments with well-defined boundary conditions [3]-[5]. In such studies, solute breakthrough curves typically are measured in the column's effluent. They provide integrated and flux-averaged information on the processes governing solute transport in the column. Time domain reflectometry has been also used to determine resident solute concentrations in a non-destructive manner both in the laboratory and in the field [6],[7]. However, this method is restricted to local measurements while the spatial resolution is therefore limited.

In a non-intrusive manner, laboratory scale experiments at different spatial scales have shown that techniques based on image analysis of dye tracer movements could be successfully used to study solute mass transport processes in porous media [8]-[11]. The objectives of this study are to determine the both longitudinal and transverse dispersivities in unsaturated porous media using image analysis linked with spatial moment analysis and to elucidate the nature of dispersion phenomena in unsaturated porous media compared to saturated porous media. A new laboratory flow-tank experiment designed to study this issue is also described in this paper.

2. SOLUTE TRANSPORT EXPERIMENTS

2.1 Materials and Methods

In the experiments, Brilliant Blue FCF is used as a dye tracer which differentiates the tracer evolution visually from the ambient pore water. The initial concentration of the Brilliant Blue FCF dye tracer was set to 1.0 mg/cm^3. Although the specific gravity of dye tracer is 1.0001 measured using the specific gravity meter and the initial concentration of tracer is determined to be low enough to avoid density-induced flow effects, there is no denying that the effect of gravity on solute transport. This dye is chosen based on good

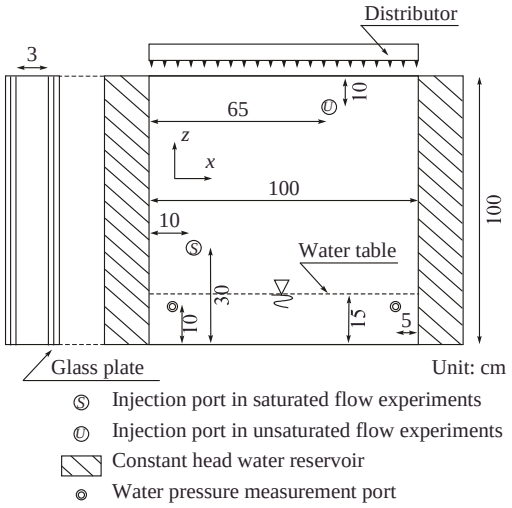

Fig.1 Schematic drawing of the experimental apparatus.

contrast with soil for visualizing transport patterns of tracer plume and low toxicity implied by its food dye designation [12].

In this study, as a soil material, silica sand with a low uniformity coefficient of 1.80 was selected in order to reflect a relatively high hydraulic conductivity fields. Silica sand of concern had 0.085 cm, 2.68 g/cm^3 and 0.751 cm/s of physical properties such as the mean particle size, the particle density and the hydraulic conductivity, respectively. Silica sand was washed and dried at 110 °C before the use to remove organic chemicals attached to the particle surface.

2.2 Solute Transport Experiments under Saturated Flow Conditions

Dye tracer experiments were carried out in a two-dimensional and vertically placed water flow tank with the dimensions of 100 cm width, 100 cm height and 3 cm thickness. The water flow tank allowed to contain soils in order to form transparent quasi two-dimensional solute transport phenomena and consisted of two glass plates with 2 cm thickness. In Fig.1, a schematic diagram of experimental apparatus is shown.

Soils were completely washed and saturated before packing to avoid entering air and to conduct experiments under the saturated condition. In the process of creation of flow field, water flow tank was filled with water and silica sand from bottom to top in 5 cm layers to achieve uniform packing. In this process, soil was funneled using an extended funnel. Each layer of interest was compacted prior to filling the next layer, resulting in 0.42 of the porosity. The porosity of each flow field was able to be estimated indirectly from measurements of the particle density and the dry soil bulk density.

After packing, water was applied to the flow tank under a specific hydraulic gradient controlled by constant head water reservoirs at the upstream and downstream sides, while maintaining saturated condition of porous media. A steady saturated flow field was established when fluctuations in the observed drainage rate, which was effluent from the constant head water reservoir, and piezometer readings could become negligible. After reaching steady state flow conditions, dye tracer with the volume of 25 cm^3, which made flow paths visible, was uniformly injected along the whole thickness of the flow tank. During the experiment, the profiles of tracer migration were periodically recorded using a digital camera, which located about 100 cm away from the front face of the water flow tank.

2.3 Solute Transport Experiments under Unsaturated Flow Conditions

Dye tracer experiments under unsaturated conditions were conducted in a similar manner. Internal drainage using constant head reservoirs allowed for approximately one day to create an unsaturated flow field after the flow tank was filled with water and silica sand. Water table was maintained at the 10 cm from the bottom of the water tank. After steady state condition was established, dye tracer with the volume of 25 cm^3 was injected in the same manner as saturated experiments. Following that, water was applied using a distributor placed 10 cm above the top of the experimental apparatus, or the ground surface, as shown in Fig.1. Three rainfall rates of 125, 190 and 290 mm/day, were set with no rainfall case. Rainfall rates employed in this study do not reflect the real rainfall situation at crop fields but are utilized as the driving force to infiltrate water and dye tracer into porous formations. In these experiments, geomembrane was placed on the ground surface to avoid the erosion due to waterdrops.

2.4 Non-Intrusive Technique Using Spatial Moment Approach and Image Processing

Each of the pixels representing an image has a pixel intensity which describes how bright that pixel is. In order to establish the relationship between the pixel intensity of a pixel and dye tracer concentration, a calibration was conducted in the same manner reported by Inoue et al. [11]. Under identical experimental conditions, a known

concentration of dye tracer was injected into a corresponding porous formation without a hydraulic gradient. The spread of dye was captured by the digital camera. The same procedure was repeated using different concentrations of dye tracer. Consequently, the concentration of the dye tracer as a function of the pixel intensity varied over the range of 0 mg/cm^3 to 1.0 mg/cm^3.

A commonly used measure of dilution is the spatial moments of aqueous concentrations, which are calculated from snapshots of tracer plume at given times as follows [13].

$$M_{ij}(t) = \int_{-\infty}^{\infty}\int_{-\infty}^{\infty} c(x,z,t)x^i z^j dxdz, \quad i,j = 1,2 \tag{1}$$

where x and z are the Cartesian coordinates, c is the solute concentration, t is the time, M_{ij} is the spatial moments associated with the distribution of tracer plume at a certain time, and i and j are the spatial order in the x and z coordinates, respectively.

The pixel intensity distribution can be converted to a concentration distribution by the calibration, providing an analogy between Eq.(1) and Eq.(2).

$$M_{ij}(t) = \int_{-\infty}^{\infty}\int_{-\infty}^{\infty} H(x,z)B(x,z,t)x^i z^j dxdz, \quad i,j = 1,2 \tag{2}$$

where $H(x,z)$ is the area per unit pixel and $B(x,z,t)$ is the intensity at a corresponding pixel. The centroid of plume concentration distribution is calculated as the normalized first order spatial moment by the following equation.

$$x_c = \frac{M_{10}}{M_{00}}, \quad z_c = \frac{M_{01}}{M_{00}} \tag{3}$$

where x_c and z_c are the centroid locations of plume concentration distribution in the x and z coordinates, respectively. The second order spatial moments are also computed as follows.

$$\sigma_{ij} = \begin{pmatrix} \sigma_{xx} & \sigma_{xz} \\ \sigma_{zx} & \sigma_{zz} \end{pmatrix} = \begin{pmatrix} \frac{M_{20}}{M_{00}} - x_c^2 & \frac{M_{11}}{M_{00}} - x_c z_c \\ \frac{M_{11}}{M_{00}} - z_c x_c & \frac{M_{02}}{M_{00}} - z_c^2 \end{pmatrix} \tag{4}$$

where σ_{ij} is the second order spatial moments.

Longitudinal and transverse dispersivities from spatial moments of the distributed tracer plume are calculated as the following Eq. (5) and Eq.(6) under saturated and unsaturated conditions, respectively [11].

$$\alpha_L = \frac{1}{2}\frac{\sigma_{xx}}{\xi_c}, \quad \alpha_T = \frac{1}{2}\frac{\sigma_{zz}}{\xi_c} \tag{5}$$

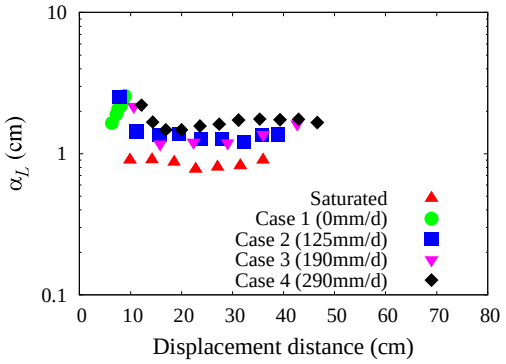

Fig.2 Results of the longitudinal dispersivity estimates.

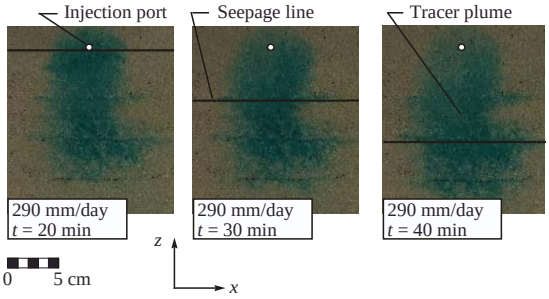

Fig. 3 Representative images of the change of dye tracer distribution.

$$\alpha_L = \frac{1}{2}\frac{\sigma_{zz}}{\xi_c}, \quad \alpha_T = \frac{1}{2}\frac{\sigma_{xx}}{\xi_c} \tag{6}$$

where α_L is the longitudinal dispersivity, α_T is the transverse dispersivity and ξ_c is the travel distance of the center of tracer plume in the mean flow direction at a given time t.

3. RESULTS AND DISCUSSION

3.1 Longitudinal Dispersivity

The results of longitudinal dispersivity α_L as a function of the displacement distance under saturated and unsaturated conditions are shown in Fig.2. Longitudinal dispersivity estimates under unsaturated conditions are two to four times larger than those under saturated conditions. The increase of the longitudinal dispersivity may be induced from diversity of solute movement due to the effect of air distribution. Several studies have pointed out the same tendency in unsaturated soils [14].

Except for the case without the rainfall intensity and under the saturated flow condition, longitudinal dispersivity estimates also exhibit a

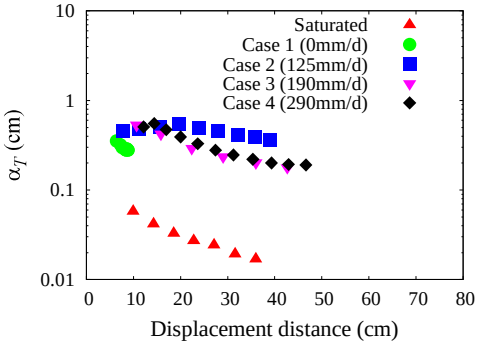

Fig.4 Relation of the transverse dispersivity estimates.

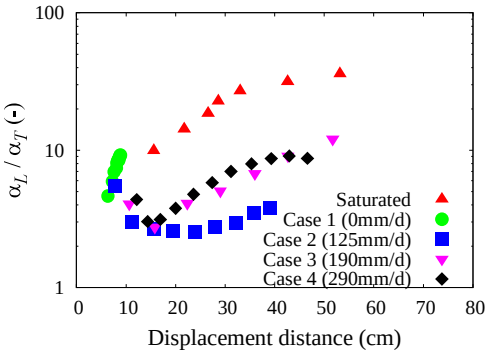

Fig.5 Results of the ratio of longitudinal to transverse dispersivities.

rapid decreasing and gradual increasing tendency and show a less dependency on infiltration rates. Water applied to the ground surface infiltrates and reaches an upper part of dye tracer. Because flow velocity is larger than solute velocity in unsaturated zone and affects the change of tracer migration patterns, shape of dye tracer distribution is shrunk longitudinally. In Fig.3, representative images of the change of dye tracer distribution are shown with seepage lines, which were visually observed through the experiments. This duration may correspond to the decreasing process of the longitudinal dispersivity due to temporarily shrunk shape of dye distribution. After infiltrating water reaches a front of dye tracer, dye tracer migrates mainly with interstitial water. However, part of dye tracer has relatively low velocities due to the effect of air entrapped within pores. Therefore, shape of dye tracer extends longitudinally, leading to the increase of longitudinal dispersivity estimates. Basically, as solutes move with interstitial water, the intensity of infiltration rates has little effect on the magnitude of the longitudinal dispersivity under the experimental conditions adopted in this study.

3.2 Transverse Dispersivity

The results of transverse dispersivity α_T as a function of the displacement distance under saturated and unsaturated conditions are shown in Fig.4. Transverse dispersivity estimates under unsaturated conditions are also larger than those under saturated conditions. Unlike the results of the longitudinal dispersivity, the values of the transverse dispersivity under unsaturated conditions more than ten times larger than those under saturated conditions. Except for the case without the rainfall intensity, transverse dispersivity estimates show a slight increase and a gradual decreasing tendency. It is inferred that transverse solute displacement depends largely on mixing of water and air whose distribution varies with the depth. As aforementioned above, the mobility of part of dye tracer may be extremely low due to the effect of air entrapped within pores. This point leads to larger values of the transverse dispersivity under unsaturated conditions.

On the contrary to the case in longitudinal dispersion phenomena under the unsaturated condition, when water applied to the ground surface reaches an upper part of dye tracer and affects the change of dye tracer distribution, a shape of dye tracer distribution extends horizontally, or laterally. This implies the increase of the transverse dispersivity as well as the decrease of the longitudinal dispersivity.

As a whole, both the longitudinal and transverse dispersivities exhibit a less dependency on infiltration rates. Although the degree of increase of water content induced from rainfall application decreases as rainfall intensity is lower, silica sand employed in this study has a relatively high hydraulic conductivity. Thus, it is inferred that the initial water distribution in the entire domain rather than the rainfall intensity influences the subsequent solute transport pathways.

3.3 Ratio of Dispersivity

The results of the ratio of the longitudinal dispersivity α_L to the transverse dispersivity α_T as a function of the displacement distance under saturated and unsaturated conditions are shown in Fig.5. For all cases, the ratio increases with the increase of the displacement distance. This indicates the shape of dye tracer distribution extends longitudinally. Under saturated condition, initial shape of dye tracer and its geometric shape strongly affect the initial value of the transverse dispersivity [11], which is relatively larger value than an inherent transverse dispersivity, or microdispersivity. According to the dye migration, the transverse dispersivity approaches to an

Table 1 Comparison of dispersivities with other experimental results.

Longitudinal dispersivity (cm)	Transverse dispersivity (cm)	Displacement distance (cm)	Condition of water content	Reference
0.78 – 0.82	0.020 – 0.060	5 – 50	Saturated	This study
0.025 – 0.10	0.005 – 0.018	35 – 60	Saturated	Inoue et al. [15]
0.522 – 0.756	–	30.2	Saturated	Maraqa et al. [16]
–	0.000039 – 0.013	30	Saturated	Robbins [17]
1.0 – 2.6	0.25 – 0.60	5 – 50	Unsaturated	This study
–	0.0029	30	Unsaturated	Massabò et al. [18]
1.02 – 1.67	0.320 – 0.577	5 – 25	Unsaturated	Inoue et al. [19]
2.6 – 18.3	0.03 – 2.20	6 - 14	Unsaturated	Abbasi et al. [20]
0.966 – 1.631	–	30.2	Unsaturated	Maraqa et al. [16]

asymptotic value. Therefore, the transverse dispersivity in Fig.4 shows an increasing tendency. On the other hand, the results under unsaturated conditions reflect the change of the degree of solute dispersion both in longitudinal and lateral directions.

3.4 Comparison with Other Studies

In order to confirm the accuracy of identified parameters, Table 1 compares the longitudinal and transverse dispersivities identified in this study with flow tank results reported in the literature that were conducted in a similar displacement distance. The results obtained in this study are in good agreement with other experimental results, although it seems that the maximum value of the longitudinal dispersivity is a slight larger value. This is probably because pulse input of dye tracer effects on the temporal change of the magnitude of the flow velocity during the short time period at the beginning of the experiments, leading to an overestimate of the longitudinal dispersivity.

4. CONCLUSIONS

In the present study, dye tracer experiments under saturated and unsaturated flow conditions have been conducted for homogeneous flow field filled with silica sand in order to investigate transport characteristics. As a non-intrusive technique, spatial moment approach linked with image analysis has applied to the estimation of not only the longitudinal dispersivity but also the transverse dispersivity in porous media. Experimental results revealed that transport parameters depend strongly on the water content where solute passes through, leading to the larger estimates under unsaturated conditions than those under saturated conditions. These estimation values agree with experimental results in the literature, indicating that employed methodology is useful to identify these transport parameters.

5. ACKNOWLEDGEMENTS

The work reported here was supported by JSPS Grant-in-Aid for Young Scientists (B).

6. REFERENCES

[1] Knobeloch L, Salna B, Hogan A, Postle J, Anderson H, “Blue babies and nitrate-contaminated well water”, Environmental Health Perspectives, Vol.108(7), 2000, pp. 675–678.
[2] Mostafalou S, Abdollahi M, “Pesticides and human chronic diseases: Evidences, mechanisms, and perspectives”, Toxicology and Applied Pharmacology, Vol.268(2), 2013, pp.157–177.
[3] Matsubayashi U, Devkota LP, Takagi F, “Characteristics of the dispersion coefficient in miscible displacement through a glass bead medium”, Journal of Hydrology, Vol.192, 1997, pp. 51–64.
[4] Vanderborght J, Vanclooster M, Timmerman A, Seuntjens P, Mallants D, Kim D-J, Jacques D,

Hubrechts L, Gonzalez C, Feyen J, Diels J, Deckers J, "Overview of inert tracer experiments in key belgian soil types: Relation between transport and soil morphological and hydraulic properties", Water Resources Research, Vol.37(12), 2001, pp.2783–2888.

[5] Javaux M, Vanderborght J, Kasteel R, Vanclooster M, "Three-dimensional modeling of the scale- and flow rate-dependency of dispersion in a heterogeneous unsaturated sandy monolith", Vadose Zone Journal, Vol.5, 2006, pp.515–528.

[6] Vanclooster M, Mallants D, Vanderborght J, Diels J, Van Orshoven J, Feyen, J, "Monitoring solute transport in a multi-layered sandy lysimeter using time domain reflectometry", Soil Science Society of America Journal, Vol.59, 1995, pp. 337–344.

[7] Weihermuller L, Kasteel R, Vanderborght J, Putz T, Vereecken H, "Soil water extraction with a suction cap: Results of numerical simulations", Vadose Zone Journal, Vol.4, 2005, pp.899–907.

[8] Jia C, Shing K, Yortsos YC, "Visualization and simulation of non-aqueous phase liquids solubilization in pore networks", Journal of Contaminant Hydrology, Vol.35(4), 1999, pp.363–387.

[9] Huang W, Smith CC, Lerner DN, Thornton SF, Oram A, "Physical modeling of solute transport in porous media: evaluation of an imaging technique using UV excited fluorescent dye", Water Research, Vol.36(7), 2002, pp.1843–1853.

[10] Jones EH, Smith CC, "Non-equilibrium partitioning tracer transport in porous media: 2-D physical modeling and imaging using a partitioning fluorescent dye", Water Research, Vol.39(20), 2005, pp.5099–5111.

[11] Inoue K, Takenouti R, Kobayashi A, Suzuki K, Tanaka T, "Assessment of a UV excited fluorescent dye technique for estimating solute dispersion in porous media", Journal of Rainwater Catchment Systems, Vol.17(1), 2011, pp.1–9.

[12] Flury M. and Flühler H., "Tracer characteristics of Brilliant Blue FCF", Soil Science Society of America Journal, Vol.59(1), 1995, pp.22-27.

[13] Freyberg DL, "A natural gradient experiment on solute transport in a sand aquifer 2. Spatial moments and the advection and dispersion of nonreactive tracers", Water Resources Research, Vol.22(13), 1986, pp.2031–2046.

[14] Vanderborght J, Vereecken H, "Review of dispersivities for transport modeling in soils", Vadose Zone Journal, Vol.6, 2007, pp.29-52.

[15] Inoue K, Kobayashi A, Matsunaga N, Tanaka T, "Application of particle tracking method to dispersivity identification and its experimental verification", Journal of Rainwater Catchment Systems, Vol.13(2), 2008, pp.7-16.

[16] Maraqa MA, Wallce RB, Voice TC, "Effects of degree of water saturation on dispersivity and immobile water in sandy soil columns", Journal of Contaminant Hydrology, Vol.25, 1997, pp.199-218.

[17] Robbins GA, "Methods for determining transverse dispersion coefficient of porous media in laboratory column experiments", Water Resources Research, Vol.25(6), 1989, pp.1249-1258.

[18] Massabò M, Catania F, Paladino O, "A new method for laboratory estimation of the transverse dispersion coefficient", Ground Water, Vol.45(3), 2007, pp.339-347.

[19] Inoue K, Setsune N, Suzuki, F, Tanaka T, "Determining transport parameters for unsaturated porous media in flow-tank experiments using image analysis", Water PollutionVIII Modelling, Monitoring and Management, WIT Press, 2006, pp.309–319.

[20] Abbasi F, Simunek J, Feyen J, van Genuchten MTh, Shouse PJ, "Simultaneous inverse estimation of soil hydraulic and solute transport parameters from transient field experiments: homogeneous soil", Transactions of the ASAE, Vol.46(4), 2033, pp.1085–1095.

Int. J. of GEOMATE, Dec, 2013, Vol. 5, No. 2 (Sl. No. 10), pp. 743-748.
MS No. 3185 received on June 14, 2013 and reviewed under GEOMATE publication policies.

Corresponding Author: Kazuya Inoue